

COOLING RATE EFFECTS ON THE METALLURGICAL RESPONSE OF A RECENTLY DEVELOPED SINTERING HARDENING GRADE

F. J. Semel
Hoeganaes Corporation, Cinnaminson, NJ 08077

**Presented at PM²TEC 2002
International Conference on Powder Metallurgy & Particulate Materials
JUNE 16 – 21, 2002 ORLANDO, FLORIDA USA**

ABSTRACT

The results of dilatometric, metallographic and hardness determinations to characterize the effects of cooling rates in the low to moderate sinter hardening range on the response of various Ancorsteel 737 SH compositions are presented.

INTRODUCTION

Ancorsteel 737 SH, a prealloyed powder for sinter hardening applications, was introduced in 1999, (1). The results of the study that accompanied its introduction as well as those of the several follow up studies that have since been reported have indicated its hardenability indirectly in terms of the mechanical properties and microstructures that are obtainable in various admix compositions under both laboratory-simulated and actual production sinter hardening conditions, (2, 3, 4, 5). However, to date, its appearance has not been supported with quantitative data that detail its response to the cooling rates typical of current sinter hardening capabilities. The purpose of the present report is to remedy this situation. The transformation temperatures, microstructures and apparent hardnesses as observed in specimens of four commonly specified Ancorsteel 737 SH compositions resulting from cooling at rates in the range from 25 to 150 °C per minute, (0.8 to 4.5 °F per second), will be presented. The Ancorsteel 737 SH compositions mentioned include two admixtures with graphite that resulted in steels containing nominal sintered carbon contents of 0.5 and 0.8 w/o and two admixtures with graphite and copper that resulted in steels nominally containing: 1) 0.6 w/o sintered carbon and 1 w/o copper; and, 2) 0.8 w/o sintered carbon and 2 w/o copper.

A survey of the P/M literature on 'Sinter Hardening', virtually from the inception of the term, approximately in 1991, (6), showed that there is as yet no standard method to assess the hardenability of either a sinter hardening powder or the admix compositions in which it is used. For the most part, the available data are similar to those mentioned above in connection with the introduction of the Ancorsteel 737 SH and thus, primarily of a qualitative nature, (7, 8, 9). Possibly, the most systematic effort so far to obtain quantitative information of the sort that would be expected of a standard procedure are those of L'Esperance et al., (10, 11). The basis of this method is an experimental setup that produces a series of cooling rates along the axis of

a cylindrical specimen that are typical of those employed in actual sinter hardening practice. For comparative purposes, the contents of the principal microstructural constituents, typically martensite and/or bainite, and the apparent hardness values as determined from cross sections of the specimen immediately adjacent to the points of temperature measurement are tabulated and/or plotted versus the cooling rates. As a practical matter, it is claimed that the results have "proved useful to establish the cooling rate and material composition required to optimize properties at the lowest cost", (12).

In spite of this apparent success, there has since been one standard procedure proposal and one request, (13, 14). In addition, Saritas et al. have recently initiated efforts to implement the well known Jominy End-Quench test as a means of assessing powder hardenability, (15). Given the considerable success of this method in the wrought steel industry, it certainly appears to have potential as a candidate P/M standard. However, it still remains to be shown that the predictive capabilities of the test will be sufficiently accurate at the relatively low cooling rates typical of sinter hardening to credit its use in actual practice.

Interestingly, although the Continuous Cooling Transformation or CCT method was cited in a number of the foregoing studies, its actual use only figured prominently in one as reported by Suzuki et al., (16). These investigators were interested in designing a sinter hardening process and needed to evaluate the effects of graphite content on the properties of parts made from a admixture that was otherwise of fixed alloy content. As a preliminary step, they chose a graphite content in the midrange of the ones targeted for study and determined just the portion of the admixture's CCT diagram that corresponded to the sinter hardening cooling rates of interest. The resulting partial diagram was then used as an effective guide to direct the balance of the study.

In the case of the present study, it was decided to use the CCT method to obtain and present the data. This decision was partly the result of the availability of dilatometric equipment with the necessary fast cool capabilities and partly the result of the foregoing findings, especially, the general indication of the literature that the method has yet to receive much attention in the context of sinter hardening. However, as it turned out, due to circumstances that arose and decisions that were taken in the course of the study, the actual method that was used here is essentially a variant of the CCT method. It differs from the latter principally in the nature of the cooling profiles to which the specimens are submitted and in the way in which the resulting data are presented. Thus, although the original intent of the investigation was specifically to obtain and present quantitative information on the sinter hardening behavior of the Ancorsteel 737 SH, it perforce turned into a study to develop a procedure to do so as well. As will be seen, the latter outcome appears to offer advantages over the currently existing procedures but is still in an early and therefore, incomplete state of development.

EXPERIMENTAL PROCEDURE

The four Ancorsteel 737 SH mix compositions that were investigated are shown overleaf in Table 1. Each was made as a laboratory bottle mix in accordance with regular admixing procedures. The graphite used was a screened grade of Asbury 3203H; the copper was ACuPowder 8081; and, the lubricant was Lonza Acrawax C. The graphite contents of the first two compositions listed were designed specifically to produce sintered carbon contents of 0.5 and 0.8 w/o respectively. The graphite contents of the remaining two mixes are as typically

specified in customer orders. As it turned out, these mixes produced sintered carbons that were just in excess of 0.6 and 0.8 w/o respectively.

Table 1 - Ancorsteel 737 SH Mix Compositions Investigated.

Mix ID	Graphite w/o	Copper w/o	Lubricant w/o
1	0.58	-	0.75
2	0.88	-	0.75
3	0.70	1.00	0.75
4	0.90	2.00	0.75

Continuous cooling dilatometry has an inherent limitation relative to sinter hardening. In sinter hardening, the work is hardened directly from the sintering temperature which, of course, is typically in excess of 1100 °C, (2000 °F). In continuous cooling dilatometry, its necessary to employ quartz refractories which are restricted to use at temperatures of no greater than about 1000 °C, (~1800 °F). Thus, it is necessary to sinter and harden specimens in separate steps. The sintering step, in the present instance, was in all cases at 1120 °C, (2050 °F), for 1/2 hour at temperature in a simulated dissociated ammonia atmosphere, (i.e. 75% H₂ and 25% N₂ by volume).

The hardening step was conducted using an horizontal dilatometer as shown schematically in Figure 1 below. Austenitizing prior to cooling for hardening was at 950 °C, (1725 °F) for 15 minutes at temperature followed by slow cooling at 10 °C per minute, (0.3 °F per second), to 850 °C, (1560 °F). The atmosphere during both the heating and cooling phases of the process was 10% H₂ and 90% He by volume at a flow rate of 1.4 liters/min., (3 cfh).

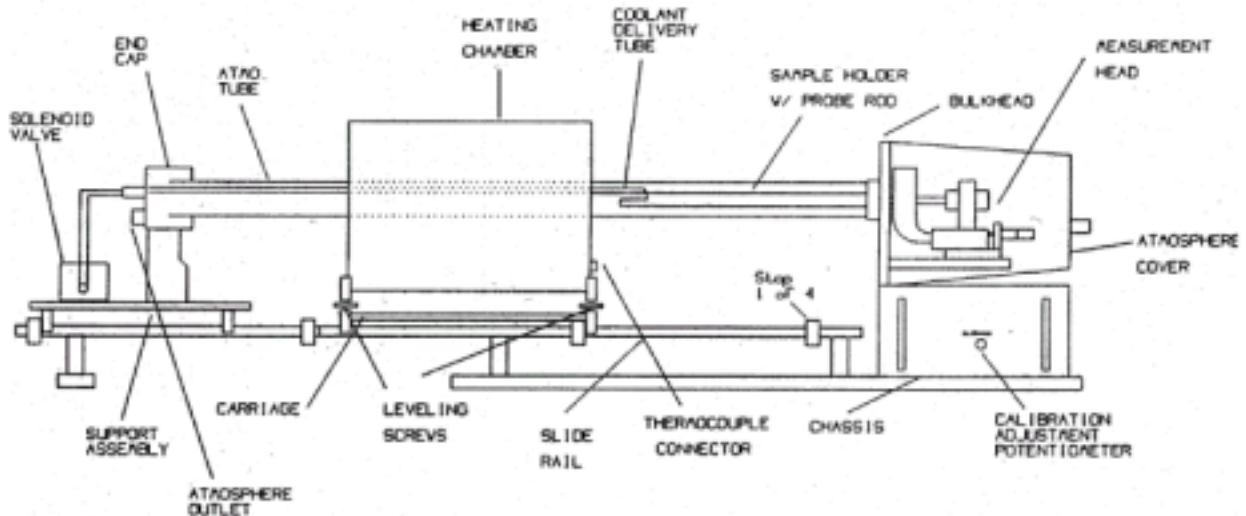


Figure 1 - Dilatometer Schematic

The essential metrical features of the dilatometer shown in the figure include a linear voltage differential transformer, (LVDT), an adjustable constant force micrometer-measuring head and a West 4400 programmable controller. The controller interfaces with thermocouples in the specimen and in the heating chamber and actuates both the power supply for heating and the solenoid relay which valves the coolant delivery tube. Time, temperature and dilation data are acquired electronically and stored digitally. The data are analyzed subsequent to acquisition in a Microsoft Excel environment using programs that were developed in this laboratory.

The position of the specimen in the unit is just downstream of the coolant delivery tube and is fixed by the design and length of the sample holder. The heating chamber, on the other hand, is on a movable carriage and may be positioned relative to the specimen anywhere along the supporting slide rail which spans the length of the atmosphere tube. The chamber itself is equipped with molybdenum di-silicide elements and is otherwise lightly insulated to permit both rapid heating and cooling of the specimen. In addition to the specimen, the sample holder and the coolant delivery tube, the atmosphere tube also houses the measuring head probe rod and the specimen thermocouple. Excluding the thermocouple, all of the latter elements and the atmosphere tube are refractory ceramics. In thermal expansion and high temperature sintering studies, the refractory of choice is alumina. However, as earlier indicated, in continuous cooling studies, quartz is required. Compared with alumina, it has an exceptionally low coefficient of expansion and as a consequence, is significantly more resistant to thermal shock.

As designed, the unit accommodates specimens with widths and heights in the neighborhood of 1 cm and lengths of from 5 to 6 cm as typical, for example, of a standard PM impact bar, (ASTM E-23). A thermocouple well is normally drilled to a depth of about 0.65 cm into the end of the specimen that interfaces with the probe rod. In thermal expansion and sintering studies, a long specimen length is an advantage because dilations are correspondingly larger and thus easier to detect. However, in continuous cooling studies, accurate determination of transition points requires the use of a relatively short specimen to minimize the magnitude of the temperature variations from the point of temperature measurement, (i.e. the bottom of the TC well). Preliminary experiments in this regard indicated that this length should be no greater than about twice the depth of the TC well, or about 1.25 cm.

Specimens of this length could easily be cut from a pressed and sintered impact bar. The difficulty, however, was to meet the requirement in the dilatometer. Two possibilities existed to do this. One was to use a non-standard probe rod to accommodate the shorter length. The other was to supplement the standard length probe rod with an inert spacer to make up the length difference. Thus, a non-standard probe rod of the required length was ordered and, in the interim, a series of trials was conducted to determine the feasibility of the spacer idea. As it turned out, a spacer in the form of a seamless 316L SS tube appeared to work rather well. In particular, it was determined that it was generally possible to separate the cooling response of the specimen from that of the spacer by comparing their combined cooling profile to one obtained under identically the same conditions but with the test specimen replaced with a stainless specimen of similar dimensions. As a consequence, it was decided to continue the investigation using the spacer and defer study of the non-standard probe rod until later. The spacer measured 4 cm in length, 1 cm in diameter, and 0.1 cm in wall thickness.

The preliminary trials also showed it was relatively easy to produce cooling rates that were typical of sinter hardening by submitting the specimen to black body radiation under different conditions of re-radiation as determined by the location of the heating chamber during the

cooling step. For example, cooling rates, determined as the average over the range from 850 to 315 °C, (1560 to 600 °F), as high as 125 °C per minute, (3.75 °F per second), or as low as 20 °C per minute, (0.6 °F per second), could be reliably reproduced using specimens that measured 1.25 cm in length, 1.1 cm in height and 1 cm in width, (i.e. as cut from an impact bar). Slightly higher rates up to 150 °C per minute, (4.5 °F per second), were possible by reducing the specimen width to 0.25 cm.

The potential to achieve even higher cooling rates by increasing the atmosphere flow rate or by using liquid N₂ as a coolant also existed but was not investigated. Instead, it was decided to base the study entirely on the radiative method as indicated. Five standard operating conditions resulting in five standard cooling rates of 27, 47, 73, 123 and 143 °C per minute, (0.8, 1.4, 2.3, 3.7 and 4.3 °F per second), were selected. Specimens of the four mix compositions were prepared from impact bars and submitted to austenitizing and hardening at each rate. The impact bars were initially compacted to green densities in the range of 7.0 to 7.05 g/cm³. Sintered densities typically varied from 6.92 to 7.0 g/cm³. Subsequent to hardening, the specimens were sectioned transverse to their longitudinal axes about 0.25 cm distance from the bottom of the TC well. The piece opposite the well was used to determine the apparent hardness and, thereafter, the sintered carbon content of the specimen. The hardness indentations were made in the face of the freshly cut section adjacent to the well. The face of the opposing section of the piece containing the well was mounted and polished for metallographic examination. The volume fractions of martensite, bainite, pearlite and ferrite were quantitatively determined as separate from the pore fraction by the point counting method. In most cases, the etchant was 4 w/o picral in reagent alcohol, (i.e. 90% ethanol by volume).

RESULTS AND DISCUSSION

Prior to presenting the hardenability findings, there are two issues that pertain to the general applicability of the procedure that are of interest. One has to do with the likely effects of the limitation imposed by the use of the quartz refractories on the magnitude of the austenitizing temperature. The other relates to the nature and probable effects of the radiative cooling method that was used.

Austenitizing Temperature

Apart from affecting the formation of austenite, the austenitizing temperature also plays a role in determining both the austenitic grain size and the extent to which alloy precipitates dissolve during the process, (17). Each, of course, affects hardenability and since the presence of undissolved precipitates can affect the grain size independently of temperature, it's appropriate to consider it first.

As a general matter, the ferrous alloying elements most likely to form precipitates, usually carbides and/or nitrides, are the more electropositive ones. In approximate order of decreasing potential in this respect, these include: niobium, vanadium, silicon, chromium, manganese and molybdenum, (18). Of these, the first two, of course, have correspondingly high affinities for oxygen and consequently are not likely to be found as other than impurities in the typical PM composition. Excluding the stainless grades which depend on a special oxidation effect, this has also been true until recently of silicon, chromium and manganese. Now, however, improved processing capabilities permit their use although, to date, only in limited amounts. Thus, the carbides and/or nitrides of these three elements and of molybdenum are of interest.

According to the available ternary phase diagrams of these elements in iron with either carbon or nitrogen, all four precipitate one or more carbides and chromium precipitates a nitride as well, (19). The diagrams also showed that the stability of the precipitates is composition dependent and, in accordance with the law of mass action, generally increases with increase in the contents of the reacting species. However, for the great majority of alloy compositions that are presently available to the P/M industry, none of the compounds other than the carbides of molybdenum were indicated to be stable at temperatures much above 800 °C, (1650 °F). In the case of the molybdenum carbides, the solution temperatures are generally higher and, in fact, at sufficiently high contents of both carbon and molybdenum can increase to values that are substantially in excess of the 1000 °C limit of the quartz refractories. However, for the more common molybdenum and carbon containing compositions, the indications were that the solution temperature is not likely to be much greater than ~900 °C, (1650 °F). For instance, the maximum solution temperature in the case of the present steels was estimated to be ~860 °C, (1580 °F). Thus, in summary, it appears that an austenitizing temperature of 950 °C, (1740 °F), as used here or a higher one up to the limit of the quartz refractories of 1000 °C, should be adequate to dissolve the alloy precipitates that are likely to occur in most PM compositions. However, such temperatures may be problematical for compositions that combine very high carbon contents with very high molybdenum contents.

In contrast with these indications, the effect of the 1000 °C temperature limit of the quartz refractories on the austenitic grain size appears to be more of a problem. As a general matter, hardenability increases with increase in the austenitic grain size and the effect is essentially independent of composition. This is because the high temperature transformation products that the hardening process is designed to prevent are heterogeneously nucleated at grain boundaries. Consequently, the larger the grain size, the smaller the resultant grain boundary area and hence, the smaller the probability that these undesirable phases, (i.e. ferrite, pearlite or bainite), will be nucleated and precipitated instead of martensite.

In the absence of grain refining precipitates, the austenitizing temperature is the principal parameter determining the grain size. Time at temperature will have some effect but since grain growth is basically a diffusion process, temperature is dominant. In sinter hardening, the austenitizing temperature is synonymous with the sintering temperature which, of course, is normally of the order of 1120 °C, (2050 °F), or higher. Thus, the dilemma posed by the temperature limitation of the quartz refractories is that the austenitizing temperature in the test will be lower than what's typical of actual practice by upwards of about 125 °C, (225 °F) or more. Based on studies conducted on wrought steels, such differences are likely to be significant in terms of their effects on both the austenitic grain size and the resulting hardenability, (20). For example, the available data indicated likely grain size differences in the neighborhood of two ASTM numbers and, depending on composition, corresponding hardenability differences as indicated by ideal diameter values of from 10 to 20%. Of course, although it remains for future studies to confirm these indications for P/M steels, the implications for the present procedure, as well as for the CCT method in general, are clear. Accordingly, such methods are likely to underestimate the hardenability in sinter hardening and, if the differences are large enough and cannot be otherwise amended, may eventually prove, in the worst case scenario, to be entirely inappropriate as a means of assessing the capabilities of the process.

Radiative Cooling

For the record, the cooling method used in these studies was not purely radiative. The flow of the protective atmosphere provided a convective component. However, whereas the effects of moderate changes in the flow were quite noticeable at low temperatures, they were not so evident at the higher temperatures. Consequently, in the temperature range from 850 to 315 °C, (1560 to 600 °F), which as will be recalled was the principal range of interest, the atmosphere's contribution to cooling is not thought to have been very significant. Of course, this is not to say that it could not be made to be significant.

The radiative cooling method is of interest because it differs significantly from the methods that are generally used in CCT determinations. According to the findings of a comprehensive review of the CCT procedure as applied to wrought steels, there are two different cooling profiles that are in common use in such determinations, (21). One is linear in which the temperature decreases directly with time and the other is so-called Newtonian in which the temperature decreases exponentially with time. In linear cooling: $T = T_o - ct$ and the average cooling rate is a constant c , independent of the temperature range over which it is measured. In Newtonian cooling: $T = T_o \cdot \exp(-ct)$ and the average cooling rate is temperature dependent. Over the range from T_o to T_f , it is given by the expression: $c(T_o - T_f)/\ln(T_o/T_f)$.

The present cooling method is similar to the Newtonian in so far as the average cooling rate that it effects is a variable function of the temperature. Otherwise, however, it is very different in terms of the cooling profiles that it produces. For example, Figure 2 shows this for an average cooling rate of 73 °C per minute, (2.2 °F per second), as determined over the earlier mentioned temperature range from 850 to 315 °C, (1560 to 600 °F). The radiative profile shown represents the average of several determinations.

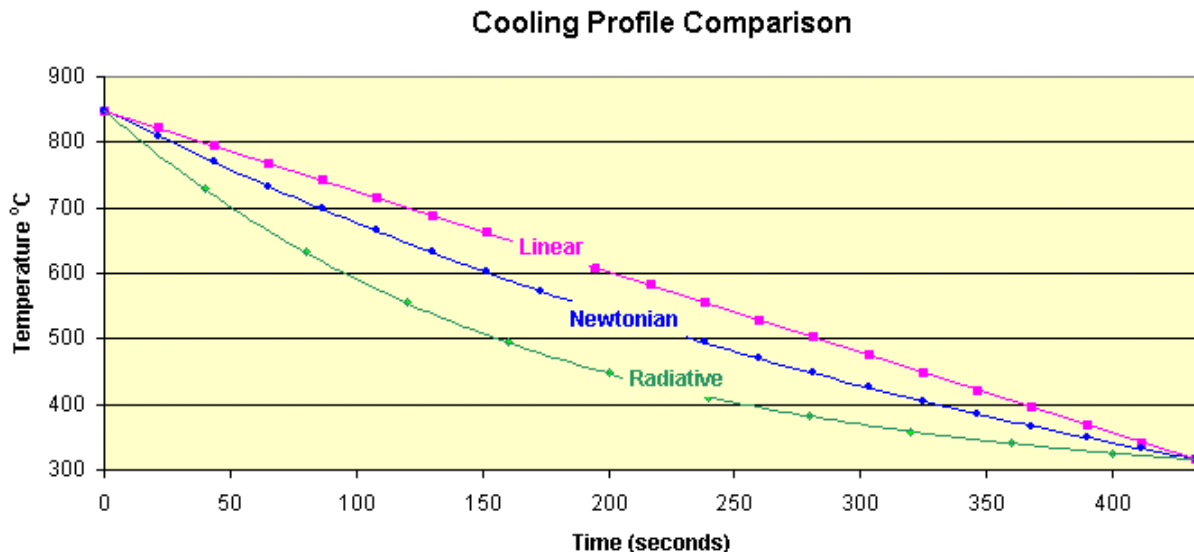


Figure 2 - Comparison of cooling profiles at an average cooling rate of 73 °C per minute.

As will be evident from the figure, the radiative profile is somewhat similar to the Newtonian in shape but is otherwise substantially different from both it and the linear profile in terms of the time-temperature relationship that it indicates. The essential difference in this regard is that the instantaneous cooling rates that it displays are comparatively higher at high temperatures and correspondingly lower at low temperatures than those of either of the latter. The findings of similar comparisons at each of the other average cooling rates of interest were basically the same.

In view of these differences, two questions immediately arise: 1) does the mode of cooling affect the hardenability and thus, the outcome of the test; and, if so, 2) which of these three modes of cooling compares most favorably with those typical of actual sinter hardening and is therefore the best mode to use in the test to simulate the process.

Theoretically, the mode of cooling should affect hardenability and hence, the outcome of the test. This is because time and temperature are the primary variables that determine the nucleation and growth of a new phase. Perhaps the prime example of this is the hardenability differences that are indicated by the Isothermal Transformation, (IT), and the CCT methods. As noted in a recent tutorial on sinter hardening, (22), and as otherwise explained in considerable detail in the aforementioned review article on the CCT method, continuous cooling displaces the transformations that are observed with isothermal cooling to lower temperatures and longer times. Thus, as a general matter, the CCT method indicates greater hardenability than the IT method and the difference is specifically traceable to the difference in the modes of cooling which are employed in the two methods.

In comparison, the radiative cooling of the present method is roughly intermediate of the two. In other words, considered over the same range of temperatures, the radiative mode results in cooling rates at high temperatures which are higher than those of the CCT method but lower than those associated with the initial quench of the IT method. Alternatively, the cooling rates that it produces at the lower temperatures of the range are lower than those of the CCT method but, of course, decidedly higher than the essentially zero rate associated with the isothermal dwell of the IT method. Thus, it is reasonable to expect that the hardenability indications of the radiative method would likewise be roughly intermediate of the those of the IT and CCT methods as well.

Data relative to the cooling profiles that are typical of sinter hardening are not generally available. However, it seems reasonable to assume that they are certainly not linear in form and very probably not Newtonian. For example, the Newtonian profile essentially reflects a constant proportionality between the temperature and its time rate of decrease which is typical of heat transfer by conduction and convection but not radiation, (23). As is generally well known, in radiation, the heat transfer varies as the fourth power of the temperature and at high temperatures is correspondingly much faster than conduction or convection or even the combination of the two. Since the whole point of cooling during sinter hardening is to minimize the time at which the work is exposed to temperatures in the range where radiative cooling is dominant, it follows that the cooling profiles typical of the process will contain a significant radiative component and thus be neither linear nor Newtonian at these temperatures. In fact, the most reasonable expectation in this regard is that they will be very like those of the radiative method.

Sinter Hardening vs Radiative Cooling

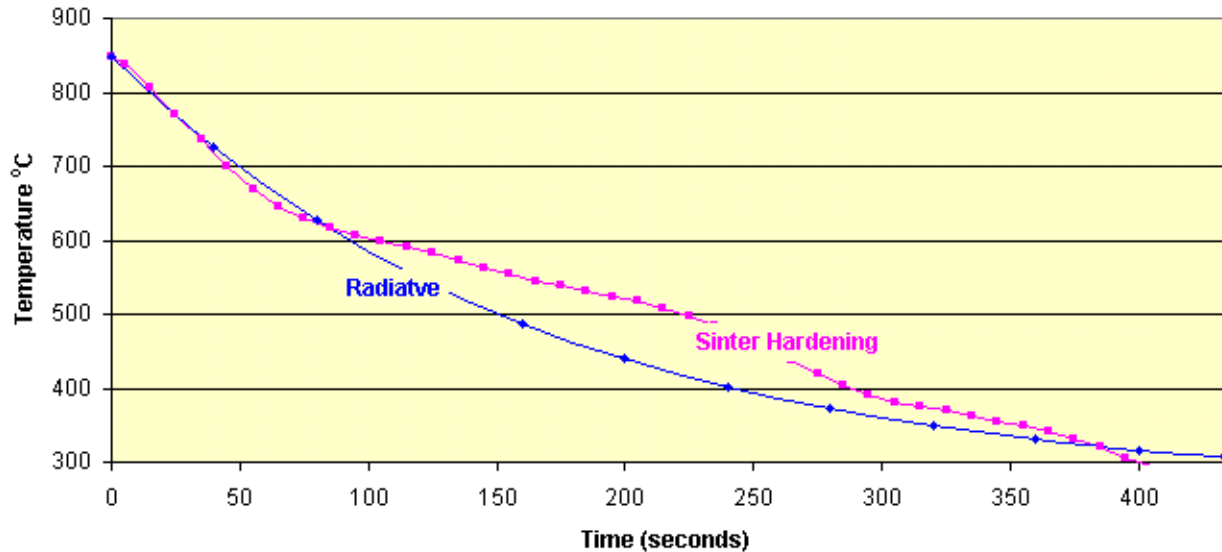


Figure 3 - Example of sinter hardening versus radiative cooling for essentially the same conditions as in Figure 2.

Significantly, limited comparisons of cooling profiles as brought about by the Abbot Varicool process that were obtained in an early study of sinter hardening tended to confirm this speculation, (24). Unfortunately, the procedure employed in this early study had yet to be perfected and was based on the cooling response of a test piece of relatively low hardenability. As a consequence, the resulting profiles were distorted by the presence of thermal recalescence due the effects of a transformation that occurred about midway through the temperature range of interest. However, the profiles nevertheless displayed a strong resemblance to the profiles of the present method in the temperature range above the point at which the transformation interrupted their progress as well as some similarity subsequent to the cessation of the transformation event. An example of these findings is shown above in Figure 3. The figure depicts essentially the same conditions of time, temperature and average cooling rate as in the earlier Figure 2.

A New Hardenability Diagram

The standard IT and CCT diagrams are extraordinarily useful devices. However, they were specifically designed for the general heat treatment of steel and not just for the hardening process. The characteristic logarithmic scheme that they employ to compress the time scale provides the potential to display a lot more information than is actually needed for the purposes of hardening and, in particular, for the purposes of sinter hardening. For example, the average sinter hardening capability typically provides a fairly narrow range of cooling rates which in terms of a diagram can be covered by a correspondingly narrow range of times. Thus, the possibility exists to present hardenability data for sinter hardening on a linear time scale. In addition, the cooling parameter that is most often cited in connection with the process is the cooling rate. Cooling rates, however, are not an integral feature of the traditional diagrams. They are occasionally included in CCT diagrams but when they are, they are always presented along with the associated cooling profile. The inclusion of the profile, of course, is an advantage

but, as it turns out, also entails a certain disadvantage. This is that the logarithmic time scale distorts the appearance of the profile to such an extent that it is not nearly as informative as it might otherwise be. For example, when linear and Newtonian profiles representing the same average cooling rate are so indicated, it is virtually impossible to distinguish one from the other.

In view of these issues, it was decided to experiment with a new type of diagram to report the present findings. Since the diagram is derived from continuous cooling data and is applicable to sinter hardening, it is referred to as a "Continuous Sinter Cooling Transformation" or CSCT diagram. Unlike the traditional diagrams, a CSCT diagram employs a linear coordinate system. The temperature axis may be graduated in degrees Celsius or degrees Fahrenheit, as protocol or common usage requires. The time axis is graduated in either seconds or minutes depending on which appears to produce the most comprehensive presentation of the findings. In addition, the diagram is prepared with the traces of, at least, three of the cooling profiles that were used to generate the data. Each is labeled as to the associated average cooling rate. Two correspond to the highest and lowest rates used and the third to cooling at an intermediate rate. As will be seen, the profiles provide a kind of superlattice for the dilatometric findings. This is because the times and temperatures corresponding to the various transformation events that the dilatometry indicates invariably plot along the length of the associated cooling profile. As in the traditional IT and CCT diagrams, phase fields are labeled in accordance with the first letter(s) of the corresponding phase(s). Finally, to make the diagram as informative as well as autonomous as possible, the results of the quantitative metallographic and apparent hardness determinations at each average cooling rate are included within its framework in the form of a text box insert.

Ancorsteel 737 SH Hardenability Results

The CSCT diagrams of the subject compositions are shown in Figures 4 through 7. As a cursory review of these findings will reveal, each of the diagrams contains phase boundaries that correspond to precipitation at both high and low temperatures. As a general matter, the dilatometric indications leading to the low temperature boundaries, (i.e. those indicating martensite and/or bainite precipitation), were consistent in the sense that the individual points defining the boundary changed position in accordance with expectation and, based on limited studies, were reasonably reproducible. However, this was not generally the case with the high temperature boundaries, (i.e. those indicating ferrite and/or pearlite precipitation). There was considerably more scatter in the dilatometric indications leading to these boundaries and the indications were not as reproducible. Thus, there is more uncertainty as to the general shape and position of these boundaries than there is in the case of the low temperature boundaries. The underlying reasons for this behavior are unknown and remain for future research to discover. Two possibilities are as follows: 1) The dilatometric procedure that was employed was flawed relative to the detection of the high temperature phases; and/or, 2) In most cases, the high temperature phases were the minor phases precipitated and as such may not have been as readily or reproducibly detectable under the best of circumstances as the low temperature phases.

In addition, it is also relevant to mention that the dilatometric data generally provided more information than is indicated in the diagrams. This was particularly true in those cases where the data indicated the precipitation of bainite followed by martensite. Generally, since the

Ancorsteel 737 SH + 0.5 w/o Sintered C at 7.0 g/cm³
Continuous Sinter Cooling Transformation Diagram

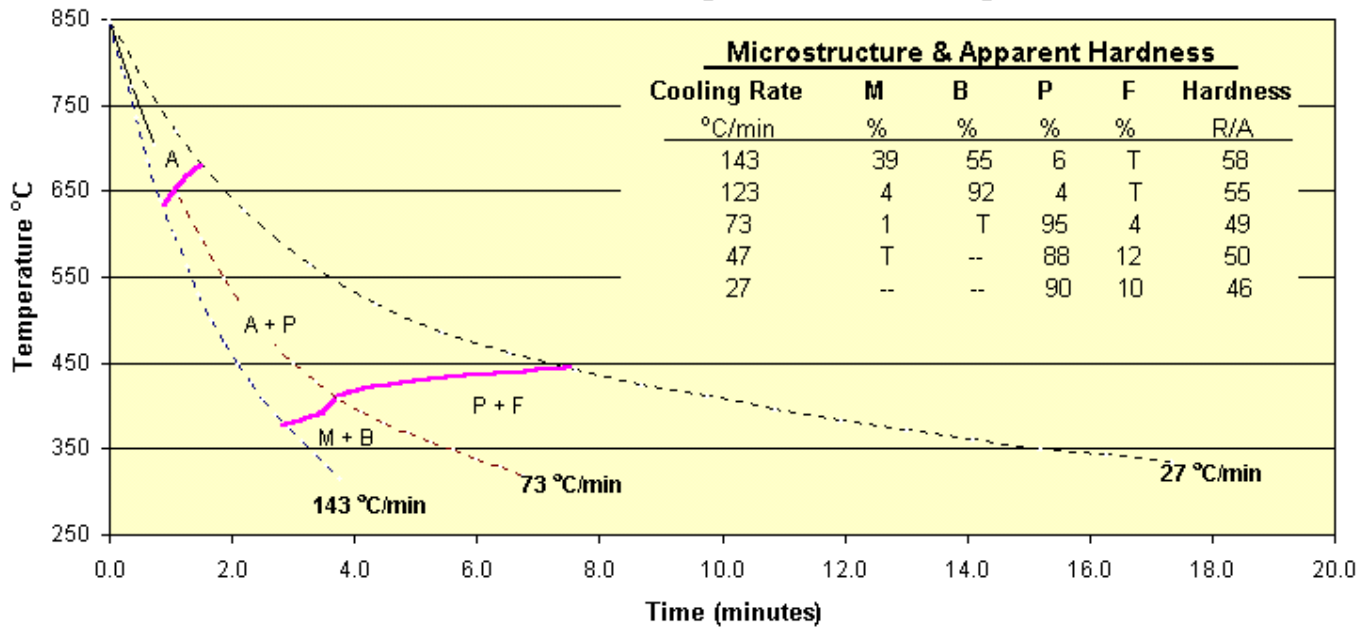


Figure 4 - CSCT Diagram of Mix 1.

Ancorsteel 737 SH + 0.8 w/o Sintered C at 6.95 g/cm³
Continuous Sinter Cooling Transformation Diagram

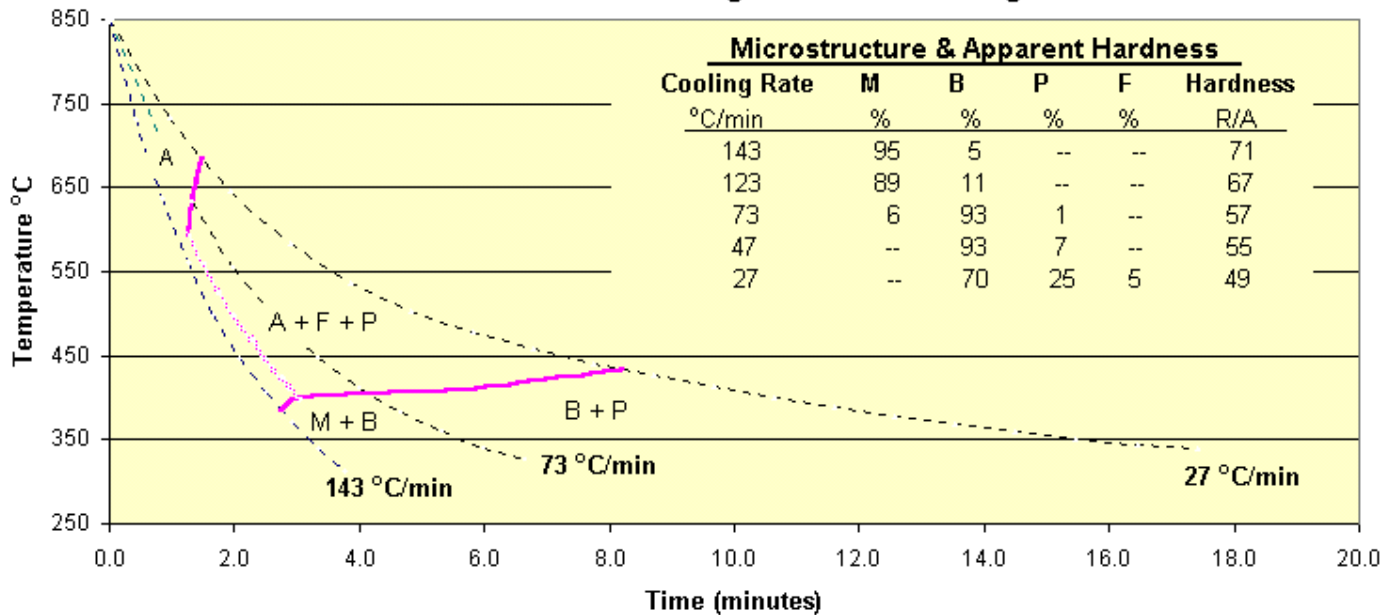


Figure 5 - CSCT Diagram of Mix 2.

metallographic results clearly show the presence of martensite in the final structure, only the bainite start temperatures are indicated in the diagram. This was done in part to keep the diagrams as simple as possible but also because the dilatometric analysis that is required to determine the martensite start temperatures in such cases is not only lengthy but yields results that have questionable value in terms of present sinter hardening capabilities.

Discussion of the hardenability results indicated by the individual diagrams follows.

Mix 1: Ancorsteel 737 SH + 0.5 w/o Sintered Carbon

The CSCT diagram of this composition is presented in Figure 4. A review of the diagram will show that it indicates that the composition's hardenability is essentially marginal. The metallographic and apparent hardness findings show that while hardness increased with increases in the cooling rate, bainite was still the principal phase observed at the highest cooling rate. The high temperature boundary indicating the precipitation of proeutectoid ferrite and/or coarse pearlite that is shown in the diagram ranges from about 630 to 670 °C, (1165 to 1240 °F). The low temperature boundary indicating the start of bainite and/or fine pearlite precipitation ranges from about 375 to 450 °C, (710 to 840 °F). As a matter of interest, the transition from bainite to pearlite that is indicated in the diagram by the labeling of the phase fields underlying this boundary is essentially a metallographic value judgement. Oftentimes, rather than make this judgement, metallographer's will simply label either or both of these phases as ferrite plus carbide.

Mix 2: Ancorsteel 737 SH + 0.8 w/o Sintered Carbon

The CSCT diagram of this composition is presented in Figure 5. A review of the diagram will show that the increased carbon content in this case over that of Mix 1 was associated with a substantial increase in hardenability. The metallographic and apparent hardness findings show an almost completely martensitic structure at the highest cooling rate and a substantially martensitic one at the next highest rate. The associated hardness values were likewise significantly improved relative to those of the lower carbon composition. The structures and hardness values at the lower cooling rates also reflected the increased hardenability. Each of the structures was predominantly bainitic whereas in the earlier mix, they were all pearlitic. The present mixes also exhibited correspondingly higher hardness values.

Interestingly, as indicated in the diagram, the first evidence of a high temperature precipitate was at the second highest cooling rate. The implication being that the "nose" of the curve indicating the onset of proeutectoid ferrite and/or coarse pearlite precipitation, in this case, is located just to the left of the cooling profile corresponding to this rate and at a temperature which is between the high and the low temperature boundaries. This is indicated in the diagram by a line that connects the boundaries along the length of the profile. The connection is drawn as a diffuse rather than a solid line to emphasize the uncertainties in its exact position and the whereabouts of the nose of the curve.

Otherwise, temperatures along the length of the high temperature boundary ranged from about 590 to 690 °C, (1095 to 1275 °F). Compared with those of the earlier composition, these temperatures cover a wider range but are centered at only a slightly lower value, i.e. 640 vs. 650 °C, (1180 vs. 1200 °F). In the case of the lower boundary, the temperatures ranged from about 375 to 430 °C, (710 to 800 °F), and were rather similar to those of the earlier steel but

**Ancorsteel 737 SH + 0.6 w/o Sintered C + 1 w/o Cu at 6.98 g/cm³.
Continuous Sinter Cooling Transformation Diagram**

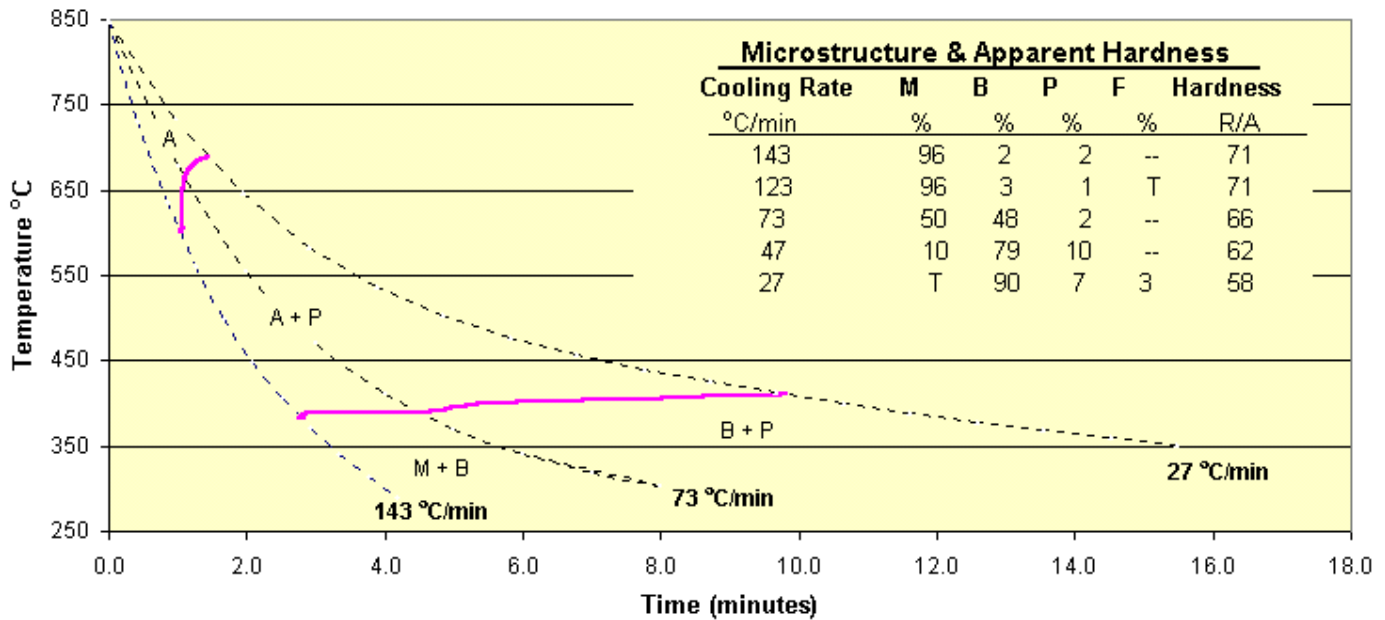


Figure 6 - CSCT Diagram of Mix 3.

**Ancorsteel 737 SH + 0.8 w/o Sintered C + 2 w/o Cu at 6.92 g/cm³.
Continuous Sinter Cooling Transformation Diagram**

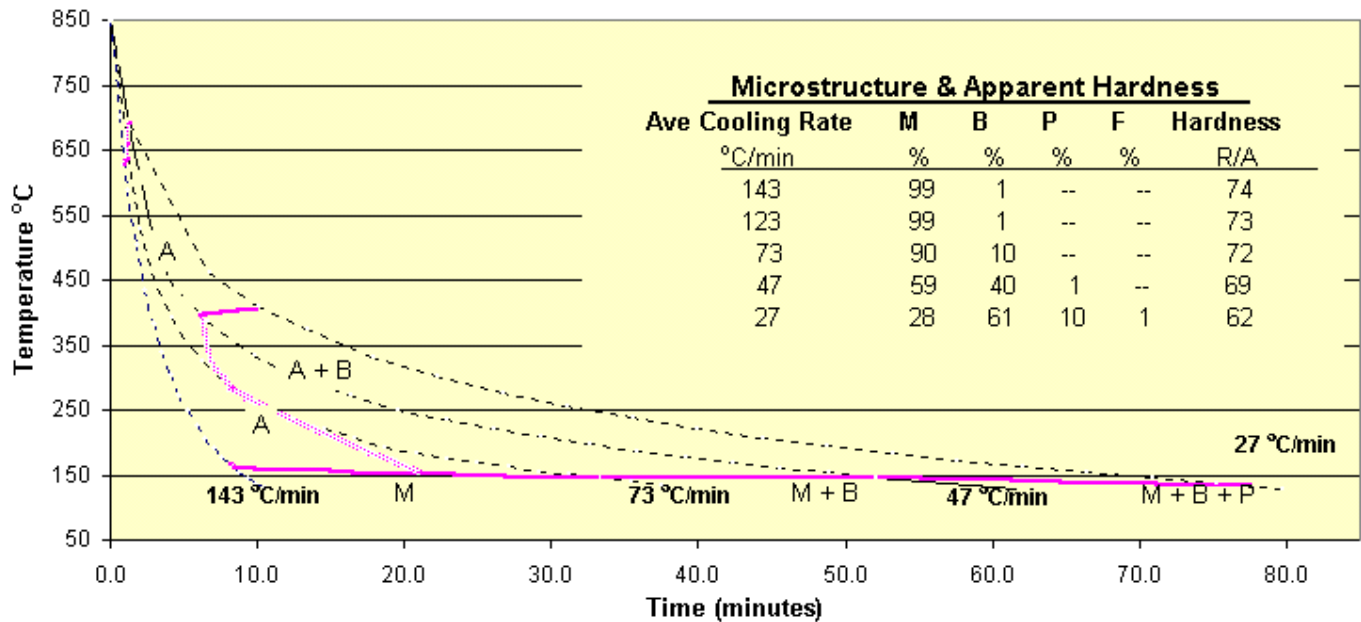


Figure 7 - CSCT Diagram of Mix 4.

were again centered ~ 10 °C, (20 °F), lower. Evidently, transformation temperatures do not always provide as good an indication of relative hardenability as do microstructure and apparent hardness.

Mix 3: Acorsteel 737 SH + 0.6 w/o Sintered Carbon + 1 w/o Copper

The CSCT diagram of this composition is presented in Figure 6. A review of the diagram will show that it is very similar in general appearance to the diagram of Mix 1 in Figure 4 and similar as well to that of Mix 2 in Figure 5; the main difference compared with the latter being the absence of the line connecting the high and low temperature boundaries. The metallographic and apparent hardness findings show that the composition is substantially better in hardenability and hardness than Mix 1 and marginally better than Mix 2.

Temperatures along the length of the high temperature boundary ranged from about 600 to 700 °C, (1110 to 1290 °F). Thus, they were similar in range to those of Mix 2 but centered about 10 °C, (20 °F), higher and hence, in this respect, similar to Mix 1. Along the length of the low temperature boundary, the range again started at ~ 375 °C, (710 °F), as in both of the earlier admixes but only increased to 410 °C, (770 °F), some 40 °C, (70 °F) below the endpoint temperature of Mix 1 and about 20 °C, (35 °F), below that of Mix 2.

Its also of interest to note that the martensite start temperatures at the three highest cooling rates were rather clearly indicated by the dilatometric data in this case. They ranged from about 220 to 300 °C, (425 to 575 °F), and increased with decreasing rate. Oftentimes, cooling rate has the opposite effect on this parameter.

Mix 4: Acorsteel 737 SH + 0.8 w/o Sintered Carbon + 2 w/o Copper

The CSCT diagram of this composition is presented in Figure 7. A review of the diagram will show that the increased carbon and copper contents in this case over those of the previous mix resulted in a substantial increase in hardenability. The metallographic and apparent hardness findings showed almost completely martensitic structures at the three highest cooling rates and a substantially martensitic one at the next highest rate. The associated hardness values were likewise improved relative to those of the earlier composition. The structure and hardness value at the lowest cooling rate also reflected the increased hardenability. Although the microstructure was predominantly bainitic as was that of the earlier steel, it contained substantially more martensite and exhibited a correspondingly higher hardness value.

Interestingly, the dilatometric findings in this case included indications of high temperature transformation products that were not supported by the metallographic results. The reasons for this are unknown and remain to be investigated. The alternatives, at this point, appear to include the following. Either the phases precipitated as indicated but were of a morphology and/or content that was not readily distinguishable from the principal phases present or they did not precipitate and the dilatometric indications relative to them were an artifact of the procedure. As a consequence, although these findings are shown in the diagram, the boundary which they indicated was drawn as a diffuse line and the phase fields adjacent it were labeled without regard for its presence. For comparative purposes, the temperatures along the length of this boundary ranged from 625 to 700 °C, (1160 to 1290 °F) and thus, were similar to those of the high temperature boundaries of the earlier diagrams.

The first evidence of significant bainite precipitation in this instance occurred at a relatively low cooling rate, i.e. at 47 °C per minute, (1.4 °F per second). As was the case with the first indications of proeutectoid ferrite and/or coarse pearlite precipitation in the earlier Mix 2, the implication was that the balance of the bainite start curve was located to the left of the cooling profile corresponding to this rate and at lower temperatures. Given the modest bainite content which the microstructural results showed at the next highest cooling rate, i.e. at 73 °C per minute, (2.2 °F per second), it was evident that prior to intersecting the martensite start boundary, the curve also crossed to the left of the cooling profile corresponding to this rate as well. Thus, as shown in the figure, the curve was sketched into the diagram so as to reflect both of these indications. Here again, it was drawn as a diffuse rather than a solid line to emphasize the uncertainty in its position.

As a final matter, the bainite start temperatures along the boundary at the top of the curve again started at 375 °C and increased with decreasing cooling rate, ranging to 400 °C, (710 to 750 °F). In contrast, the martensite start temperatures that are indicated along the lower boundary in the diagram ranged from 165 to 135 °C, (330 to 275 °F) and decreased with decreasing cooling rate.

SUMMARY AND CONCLUSIONS

The sinter hardening responses, in terms of the transformation temperatures, microstructures and apparent hardnesses, of four Ancorsteel 737 SH compositions to cooling rates in the range from 25 to 150 °C per minute, (0.8 to 4.5 °F per second), were presented. The compositions studied included two mixtures with graphite that resulted in steels containing sintered carbon contents of 0.5 and 0.8 w/o and two with graphite and copper that resulted in one steel with a sintered carbon of 0.6 w/o and a copper of 1 w/o and, a second, with a sintered carbon of 0.8 w/o and a copper of 2 w/o.

The specimens were processed in a dilatometer using a continuous cooling transformation procedure. Of necessity, the dilatometer was equipped with quartz refractories which limited the maximum austenitizing temperature to 1000 °C, (1830 °F). Since the austenitizing temperatures in sinter hardening are typical of sintering and therefore of the order of 1120 °C, (2050 °F), or higher, this limitation raised two concerns. One had to do with the possible effects on the solution of alloy precipitates and the other with the effects on the austenitic grain size, both of which can affect hardenability. Literature surveys relative to each indicated that while temperatures of less than a 1000 °C would be adequate to dissolve the alloy precipitates that occur in the great majority of P/M steels, they were also likely to be significantly limiting in terms of the effects on the austenitic grain size and thus, on the hardenability results indicated by the procedure. Thus, the implication for the continuous cooling procedure in general was that it may have limited applicability for assessing hardenability for sinter hardening purposes. The specific implication for the present study was that the results should be looked upon as being essentially conservative estimates of the hardenabilities of the subject compositions.

Cooling in accordance with the experimental procedure that was used was principally by radiation. It was shown that the resulting cooling profiles differed from the linear and Newtonian profiles that are normally employed with the CCT method and it was noted that this was potentially important because the nature of the cooling profile is likely to affect the hardening response and thus, both the outcome of the test as well as the results of any hardening operation that the test aims to guide. Theoretical considerations were presented which led to

the speculation that the cooling profiles typical of actual sinter hardening are likely to be similar to the radiative profiles under discussion and limited experimental evidence was subsequently presented that supported this idea.

Instead of using the traditional CCT diagram to present the hardenability findings, it was decided to try a new presentation called a Continuous Sinter Cooling Transformation or CSCT diagram. The CSCT diagram differs from the traditional one in three ways. First, it uses a linear time scale rather than a logarithmic one. Second, the traces of at least three of the cooling profiles that were used to generate the findings are included in the diagram to provide an additional framework to log the transformation temperatures and times. Last, the metallographic and apparent hardness results corresponding to each of the cooling rates used are also entered into the diagram in the form of a text box insert.

The hardenability results of the four Ancorsteel 737 SH mixes were accordingly presented in CSCT diagrams. In general, these findings showed that transformation temperatures decreased and hardenability as indicated by microstructure and apparent hardness increased with increasing alloy content. Mix 1 with a sintered carbon content of 0.5 w/o exhibited marginal hardening responses and apparent hardnesses. The microstructure was principally bainitic at the highest cooling rates and transitioned to fine pearlite at the lower rates. Mix 2 with a sintered carbon content of 0.8 w/o exhibited substantially higher hardenability including higher apparent hardnesses. The structure was principally martensitic at the highest cooling rates and transitioned to bainite and thereafter to mostly bainite with some fine pearlite at the lower rates. Mix 3 with a sintered carbon of 0.6 w/o and a copper of 1 w/o exhibited about the same hardenability in terms of structure as Mix 2 but higher apparent hardness values at every cooling rate. Last, Mix 4 with a sintered carbon of 0.8 w/o and a copper of 2 w/o exhibited the best overall hardening responses of the study. Its microstructure was completely martensitic at the highest cooling rates and predominantly martensitic at all but the lowest rate. For comparable conditions, its apparent hardness values were substantially higher than those of Mixes 1 and 2 and moderately higher than those of Mix 3.

Finally, it is of interest to note that a review of the CSCT diagrams of the first three mixes as presented in Figures 4 through 6 will show that the transformation behaviors which they indicate are all very similar. Given the fact that their actual hardening responses, as shown by the microstructure and apparent hardness results, were otherwise all very different, it seems reasonable to conclude that transformation data per se do not generally provide an adequate indication of hardenability. However, this is not to say that such data are not helpful or possibly, even essential. For example, returning to the same three diagrams, the transformation data make it possible to tell at a glance that none of these alloys will be through hardening at the indicated cooling rates whereas in the case of the CSCT diagram in Figure 7, they similarly show that Mix 4 will be through hardening, at least, at the highest cooling rates.

ACKNOWLEDGEMENTS

The author wishes to acknowledge the help of Messrs. W. B. Bentcliff, G. Golin and T. Murphy of the Hoeganaes Laboratory in obtaining the data used in preparing the present manuscript.

REFERENCES

- 1) M. C. Baran, A. H. Graham, A. B. Davala, R. J. Causton and C. Shade, "A Superior Sinter Hardenable Material", *Advances in Powder Metallurgy & Particulate Materials*, Vol. 2, Part 7, Metal Powder Industries Federation, Princeton, N J, 1999 pp. 185.
- 2) M. C. Baran and T. Prucher, "Application of Sinter Hardenable Materials for Advanced Automotive Applications such as Gears, Cams, and Sprockets", *Society of Automotive Engineers*, Detroit, MI, 2000, Paper No. 2000-01-0999.
- 3) T. J. Miller, J. Groark, R. J. Causton and A. B. Davala, "Improved Efficiency by Use of Sinter Hardened P/M Automotive Components", *Society of Automotive Engineers*, Detroit, MI, 2000, Paper No. 2000-01-0406.
- 4) T. E. Haberberger, T. J. Cornelio, M. C. Baran and P. J. Winterton, "Field Experience on a New Sinter Hardenable Material", *Advances in Powder Metallurgy & Particulate Materials*, Part 10, Metal Powder Industries Federation, Princeton, N J, 2000 pp. 10-101.
- 5) T. E. Haberberger, M. C. Baran and F. Hanejko, "Advanced Processing of Sinter Hardening Materials" *Advances in Powder Metallurgy & Particulate Materials*, Part 5, Metal Powder Industries Federation, Princeton, N J, 2001 pp. 5-9.
- 6) R. J. Causton, and W. J. James, "Performance Characteristics of a New Sinter Hardening Low Alloy Steel", *Advances in Powder Metallurgy & Particulate Materials*, Vol. 5, Metal Powder Industries Federation, Princeton, N J, 1991, pp. 91.
- 7) J. J. Fulmer, "Sinter Hardening Steels Effect of Prealloyed Steel Powder Composition on Mechanical Properties", *Advances in Powder Metallurgy & Particulate Materials*, Vol. 6, Metal Powder Industries Federation, Princeton, N J, 1994, pp. 175.
- 8) F. Chagnon and Y. Trudel, "Designing Low Alloy Steel Powders For Sinter Hardening Applications", *Advances in Powder Metallurgy & Particulate Materials*, Vol. 4, Part 13, Metal Powder Industries Federation, Princeton, N J, 1996, pp. 13-211.
- 9) U. Engstrom, "Evaluation of Sinter Hardening of Different PM Materials", *Advances in Powder Metallurgy & Particulate Materials*, Part 5, Metal Powder Industries Federation, Princeton, N J, 2000, pp. 5-147.
- 10) G. L. 'Esperance, S. Harton, A. de Rege and S. Nigarura, "Evaluation of the Hardenability, Microstructure and Properties of Various Sinter Hardening Alloys", *Advances in Powder Metallurgy & Particulate Materials*, Vol. 8, Metal Powder Industries Federation, Princeton, N J, 1995, pp. 8-3.
- 11) G. L. 'Esperance, E. Duchesne and A. de Rege, "Effect of Materials and Process Parameters on the Microstructure and Properties of Sinter Hardening Alloys", *Advances in Powder Metallurgy & Particulate Materials*, Vol. 3, Part 11, Metal Powder Industries Federation, Princeton, N J, 1996, pp. 11-397.
- 12) H. Ferguson, G. L. 'Esperance, E. Duchesne and A. de Rege, "Effect of Mass/Cross Sectional Thickness on Sinter Hardening of Two Prealloyed Steels of Different Hardenability", *Advances in Powder Metallurgy & Particulate Materials*, Vol. 2, Part 14, Metal Powder Industries Federation, Princeton, N J, 1997, pp. 14-67.
- 13) M. A. Pershing and H. Nandi, "A Methodology for Evaluating Sinter Hardening Capability", *Advances in Powder Metallurgy & Particulate Materials*, Part 5, Metal Powder Industries Federation, Princeton, N J, 2000, pp. 5-26.
- 14) M. C. Thomason, "Sintering Furnace Cooling Method Study", *Advances in Powder Metallurgy & Particulate Materials*, Part 5, Metal Powder Industries Federation, Princeton, N J, 2000, pp. 5-103.

- 15) Saritas, R. D. Doherty and A. Lawley, "Effect of Porosity on the Hardenability of P/M Steels", *Advances in Powder Metallurgy & Particulate Materials*, Part 10, Metal Powder Industries Federation, Princeton, N J, 2001, pp. 10-112.
- 16) H. Suzuki, M. Satoh, M. Yoshida, Y. Seki, "Sinter Hardening Properties of Prealloyed Powder, 46F3H", *Advances in Powder Metallurgy & Particulate Materials*, Part 5, Metal Powder Industries Federation, Princeton, N J, 2000, pp. 5-125.
- 17) *Atlas of Isothermal Transformation Diagrams*, Second Edition, United States Steel Company, Pittsburgh, Pa, 1951, pp. 129.
- 18) L. S. Darken and R. W. Gurry, *Physical Chemistry of Metals*, McGraw-Hill Book Co., New York, 1953, pp. 349.
- 19) *Metals Handbook*, Eighth Edition, 1973, Vol. 8, "Metallography, Structures and Phase Diagrams", American Society of Metals, Metals Park, OH, pp. 402-415, 423.
- 20) E. C. Bain and H. W. Paxton, *Alloying Elements In Steel*, Second Edition, American Society of Metals, Metals Park, OH, 1952, pp. 159-169.
- 21) G. T. Eldis, "A Critical Review of Data Sources for Isothermal Transformation and Continuous Cooling Transformation Diagrams", *Hardenability Concepts with Application to Steel*, D. V. Doane and J. S. Kirkaldy, Editors, AIME/ASM, 1977.
- 22) W. B. James, "What Is Sinter Hardening?", Special Session Presentation: *International Conference on Powder Metallurgy & Particulate Materials*, Las Vegas, NV, 1998.
- 23) M. Jakob and G. A. Hawkins, *Elements of Heat Transfer*, Third Edition, John Wiley & Sons, New York, 1958, pp. 2-3.
- 24) Private Communication, R. J. Causton, Hoeganaes Corporation, Cinnaminson, NJ.